Thermal Shock Resistance of ZrO_2-8wt.%Y_2O_3 Coatings Prepared by Plasma Laser Hybrid Spraying Technique[†]

Sang Ok CHWA* and Akira OHMORI**

Abstract

Thermal spraying techniques have been widely applied for the production of ceramic protection layers on metals used in various hostile environments. However, all sprayed coatings have defects such as connected pores and unmelted particles,which deteriorate coating properties. To improve the properties of sprayed coatings, many approaches have been undertaken, such as laser irradiation, seal sintering with liquid alloys and sol-gel infiltration techniques. Lasers are promising technological tools due to speedy treatment and simplicity of process control. Moreover, laser treatment technology enables not only the post-treatment but also the pre and simultaneous treatment by combining with spraying process. TBC consisting of yttria partially stabilized zirconia layer and MCrAlY bond coating have been widely used to improve the performance of hot-section components used in gas turbines. To improve the lifetime of TBC coatings, post treatments of sprayed coatings and simultaneous spraying processes by plasma laser hybrid technique were tried. A technique using a low-viscosity resin with a fluorescent dye under a high vacuum has been tried for the accurate observation of microstructure of TBC coatings prepared by post laser treatments and laser hybrid spraying process. As a result of water quenching tests, coatings prepared by post laser treatments and laser hybrid spraying processes showed significantly improved thermal shock resistance compared with as-sprayed coatings. The relation of thermal shock resistance and microstructure of TBC coatings were evaluated by the careful observation of samples prepared by a vacuum infiltration technique with a low-viscosity resin and a fluorescent die.

KEY WORDS: (Plasma Spraying) (Laser Hybrid Technique) (TBC Coating)(Thermal Shock Resistance) (Microstructure) (Low Viscosity Spurr Resin) (Confocal Laser Scanning Microscopy)

1. Introduction

TBC consisting of yttria partially stabilized zirconia (YPSZ) layer and MCrAlY bond coating have been widely used to improve the performance of hot-section components used in gas turbines.[1-3]

To enhance the lifetime of TBC coatings under thermal shock, treatments such as post laser irradiation and laser hybrid spraying have been tried, and showed that the segmented cracks in coatings induced by laser treatment improved the thermal shock resistance.[4-7]

However, the microstructures of TBC coatings prepared by post treatment of laser or plasma laser hybrid spraying process are not clear because the conventional laser, itself has a non-uniform energy distribution in laser treatment. To obtain a near-uniform beam intensity, a kaleidoscope was installed in a conventional YAG laser, and laser treatment was carried out by combining it with the spraying process.

Another uncertain understanding of microstructure of TBC coatings prepared by post treatment of the laser and plasma laser hybrid spraying process comes from the sample preparation process for the observation of microstructures in TBC coatings. Because the mechanical stresses that arise during the mounting, cutting, grinding, and polishing operations can result in material pullout, these alter the structural features of segmented microcracks and damage the specimen.[8]

In this research, a technique using a low-viscosity resin with a fluorescent dye under a high vacuum has been tried for the accurate observation of microstructure of TBC coating prepared by post laser treatments and laser hybrid spraying process, to investigate the relation of microstructure and thermal shock property of TBC coating.

2. Experimental Details

2.1 Laser Combined Plasma Spraying System

Post treatments of predeposited coatings and simultaneous treatments during the spraying process were carried out using the laser combined spraying system. Both plasma gun (SG-100 model, Miller Thermal, Appleton, WI, USA) and the laser gun were installed inside a chamber equipped with a exhaust system. An Nd:YAG laser (NEC, Sagamihara, Kanagawa, Japan) working in continuous wave mode at 1.06 μm was used and the laser beam coming from the oscilator was delivered by optical fiber to the laser nozzle. The samples for the laser treatment were fixed onto an X-Y table, moved by a six-axes articulated robot. The details of the plasma spraying system combined with conventional-laser can be found in our previous report.[9] To obtain a uniform beam intensity, a kaleidoscope composed of two pairs of gold mirror (3.6×51 mm^2) was installed in a conventional YAG laser. The schematic diagram of a YAG laser gun equipped with a kaleidoscope is depicted in **Fig. 1**.
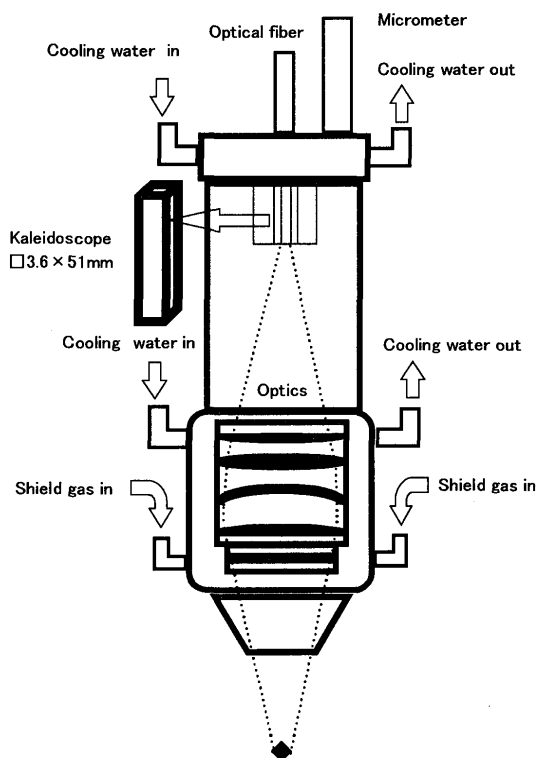

Fig. 1 Schematic diagram of YAG laser gun equipped with a kaleidoscope.

The beam delivered by an optical fiber is reflected many times on internal reflective metal walls and emerges well homogenized through the optics. The beam characteristics of the YAG laser were analyzed by laserscope UFF100 and laser beam powermeter (Prometec, Achen, Germany). The beam size of kaleidoscope-installed YAG laser varied from 5×5 mm^2

to 15×15 mm^2 by adjusting the distance between the optics and kaleidoscope with a micrometer. Beam profiles of kaleidoscope-installed YAG laser at the exit of nozzle are characterized by "top-flat" distribution. The usefulness in laser treatment using the kaleidoscope can be found in our previous report.[7]

2.2 Materials and Laser Treatment Conditions

Thermal barrier coatings consisting of 8wt% yttria partially stabilized zirconia layer and NiCrAlY bond coating were plasma sprayed on sandblasted JIS SUS304 steel with commercially available powders (Showa Denko, Shijiri, Nagano, Japan). Before plasma spraying of YPSZ, a heat resistant NiCrAlY bond coating of approximately 100 μm thickness was prepared at a pressure of 13.30 kPa argon gas atmosphere. **Table 1** summarizes the plasma spraying parameters and **Table 2** shows the post-laser irradiation and plasma-laser hybrid spraying conditions of YSZ coating, respectively. For the plasma spraying, a small diameter of 5 mm nozzle was used to increase overlapping with the laser beam during the plasma-laser hybrid spraying process.

Table 1 Plasma spraying parameters

Process parameters	NiCrAlY	ZrO_2-8wt.%Y_2O_3
Primary gas (Ar), m^3/s	4.17×10^{-4}	4.17×10^{-4}
Secondary gas (N_2), m^3/s	-	6.7×10^{-5}
Current/Voltage (A/V)	600/45	600/47
Spray distance (mm)	150	100
Atmosphere (kPa)	13.3	101.3

Table 2 Post-laser treatment and plasma-laser hybrid Conditions

Process parameters	Post-laser treatment	Plasma-laser hybrid treatment
Laser power (kW)	1～4	1～4
Spot size (mm^2)	(5×5～12×12)	(5×5)
Scan speed (mm/sec)	10	250
Overlap (mm)	0～2	1

2.3 Sample preparation for the CLSM observation

2.3.1 Vacuum impregnation

For the observation of the microstructure of as-sprayed and laser-treated coatings, Spurr resin with a very low viscosity of 60 cps was used as a imbedding material for vacuum impregnation. Unlike the other epoxies, Spurr resin, retains a low viscosity during heating to sufficiently penetrate the TBC coating prior to the full curing of specimen. The Spurr resin is based on the four following components (Aldrich, Milwaukee, WI, USA);vinylcyclohexene oxide (VCD), diglycidyl ether of polypropylene glycol (D.E.R. 736), nonenyl succinic anhydride (NSA), dimethylaminoethanol (DMAE). The medium was prepared by weighing the components singly into a tared disposable plastic beaker and amount of each component was based on the technical sheet of the supplier for optimum performance. The DMAE was added last after gently mixing other components. Fluorescent dye, Epodye (Struers, Westlake, OH, USA) was also added for the usage of the observation by confocal laser scanning microscope (CLSM). The resin mix was poured over the specimen mounted in a mould, and then placed in a vacuum oven with a rotary pump. After pumping about one hour to reach the pressure of 10^{-2} Pa, the vacuum was broken and vented to atmospheric pressure to accelerate the infiltration of resin, and this procedure was repeated three times. Finally, the sample was cured at 345K for 48 hours. After curing, the samples were ground and polished for CLSM observation.

2.3.2 Confocal Laser Scanning Microscopy

Observation was carried out with a CLSM (LSM410 model, Carl-Zeiss, Oberkochen, Germany) equipped with an argon-krypton laser. The principle of this equipment is to collect, by means of a pin-hole(variable diameter diaphragm) situated in front of the detector, reflected, diffracted, and fluorescent rays coming from the focal plane of the objective lens.[10] Any other part of the beam coming from other focal planes is limited and dose not contribute formation of the image. The pinhole scans the x-y surface of the sample. This microscope can visualize optical z-sections of the fluorescent resin paths through the specimen and build up a three-dimensional reconstructed image. The depth of the observed volume depends on the movement of the microscope along the z-direction. Three dimensional images are obtained by cutting optically the sample with the laser penetration at selected Δz; each section being digitally stored and finally reconstructed. There is no need to mechanically section the sample, and therefore no mechanical deformation affects the measurements.

2.4 Thermal shock test

The thermal shock resistance of a laser-treated YSZ

sample was evaluated by the following method. The substrates of plasma spraying for the thermal shock test were machined to have same tapered edges as shown in **Fig. 2**. The specimen was kept in the furnace for 3 minutes after reaching test temperature (1273 K) and then dropped into icy water(279 ± 2 K). After each thermal cycle, the sample was visually observed. Testing was stopped when the TBC coat spalled from 50% of the test zone (20×20 mm^2).
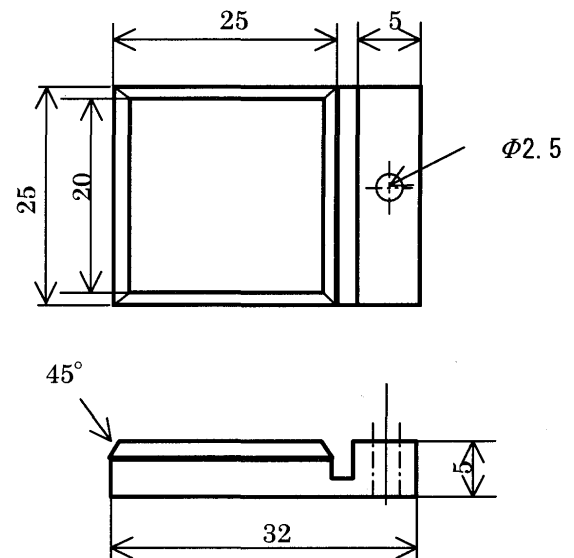

Fig. 2 Shape of substrate used for the thermal shock test

3. Results and discussions

3.1 Microstructure of coatings

Fig. 3 show a CLSM image of a plasma sprayed coating prepared by vacuum impregnation of fluorescent modified Spurr resin. **Fig. 3(a)** shows images of 9 x-y sections obtained by cutting optically the sample with a step of selected Δz (3μm) and **Fig. 3(b)** is a finally reconstructed image from the stored images of **Fig. 3(a)**. As can be seen in the **Fig. 3(b)**, the fluorescent resin is observed deep inside the coating and reaches to the interface of bond coat and top coat, revealing a large number of pores with a different sizes.

When the coating contains very fine defects and microcracks, it is difficult to differentiate between original defects formed by the spray process and induced ones from metallographical procedures. Other methods for impregnation by metals of their salts may also be used. However, the main practical disadvantage is that it is impossible to get a three dimensional image. Vacuum infiltration technique with a fluorescent modified Spurr resin is considered to be a very effective way of visualizing the three dimensional structure.
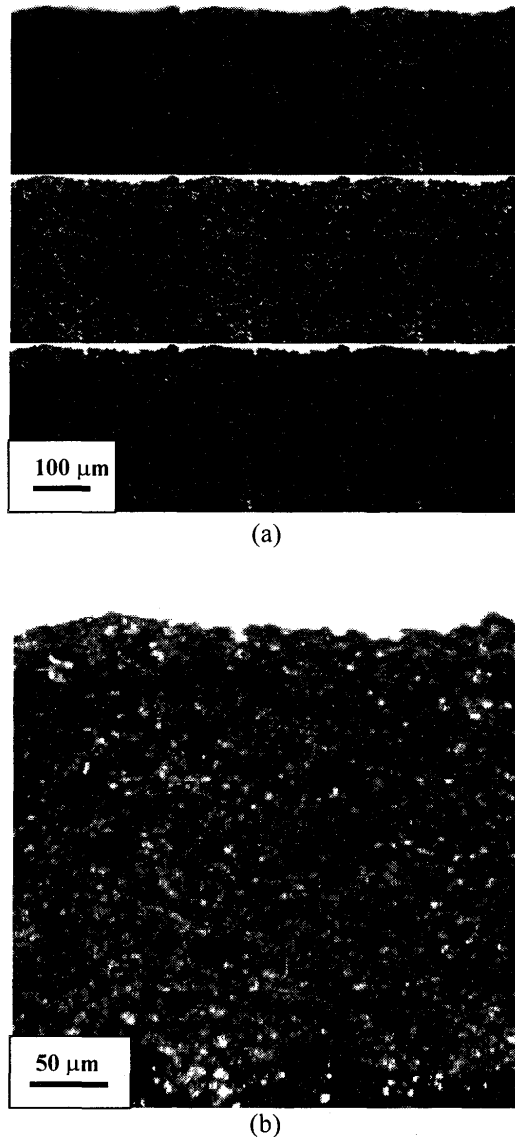
vertical cracks were generated by the relaxation of residual stress during the cooling down of molten zirconia to room temperature. Melted depth was about 50μm, and treated layer was very dense with no resin infiltration even in vacuum impregnation treatment. Depth and width of cracks increased with increasing power from 1 to 1.5kW, and very smooth surface was obtained.
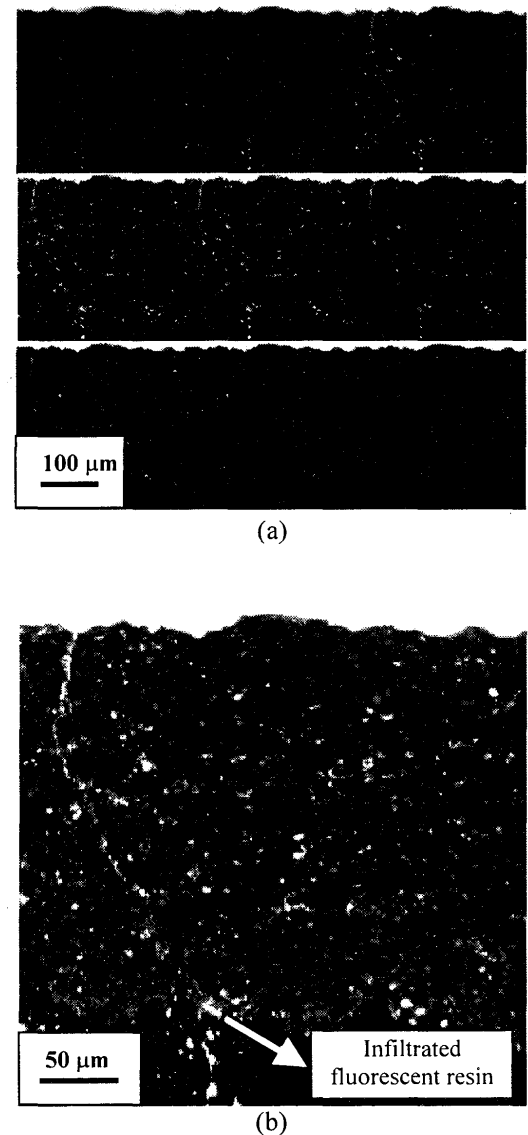

Fig. 3 (a) CLSM series of 9 x-y optical sections of as-sprayed YPSZ coating; (b)three-dimensional reconstruction of Fig.3(a) corresponding to a volume of 320 by 320 by 18 μm^3

For the treatment of 1kW laser power with kaleidoscope (Fig. 4(a) and Fig. 4(b)), pores in the surface region decreased and microcracks generated though the boundaries of splats were observed. When the treated surface of specimen was examined, no glazing from a laser treatment was observed. Therefore, the reduced porosity and microcracks are considered to result from sintering between sprayed splats without remelting of coating. With the laser power of 1.5 kW with a kaleidoscope, remelting of sprayed coating occurred and resulted in formation of the vertical cracks extending to the interface between the bond coat and top coat as shown in the Fig. 5(a) and Fig. 5(b). The

Fig. 4 (a) CLSM series of 9 x-y optical sections of laser-treated YPSZ coating (laser power: 1kW, beam size: □ 7 × 7mm²); (b)three-dimensional reconstruction of Fig.4(a) corresponding to a volume of 320 by 320 by 18 μm^3

When the laser power was increased to 2.0 kW, large bubbles were found in the coating as shown in the Fig. 6(a) and Fig. 6(b). Y. Fu et al. also reported this phenomenon and explained the bubble formation mechanism as follows.[11] when the as sprayed coating

is remelted by laser, with a flow of argon shield gas, the pores in the as-sprayed coating, (which initially have a similar size and are evenly distributed), begin to coalesce into large voids and tend to rise to the surface. Bubbles can occasionally be formed because of the involvement of some argon gas in the coating. As the laser beam moves away from any molten area with considerable speed, the molten coating solidifies rapidly. Some of the newly formed larger bubbles escape from the melting pool, while the remainder are trapped in the quenched melting pool. During the rapid solidification of the remelted coating, higher thermal stress causes the formation of cracks, and some cracks pass through the larger bubbles.
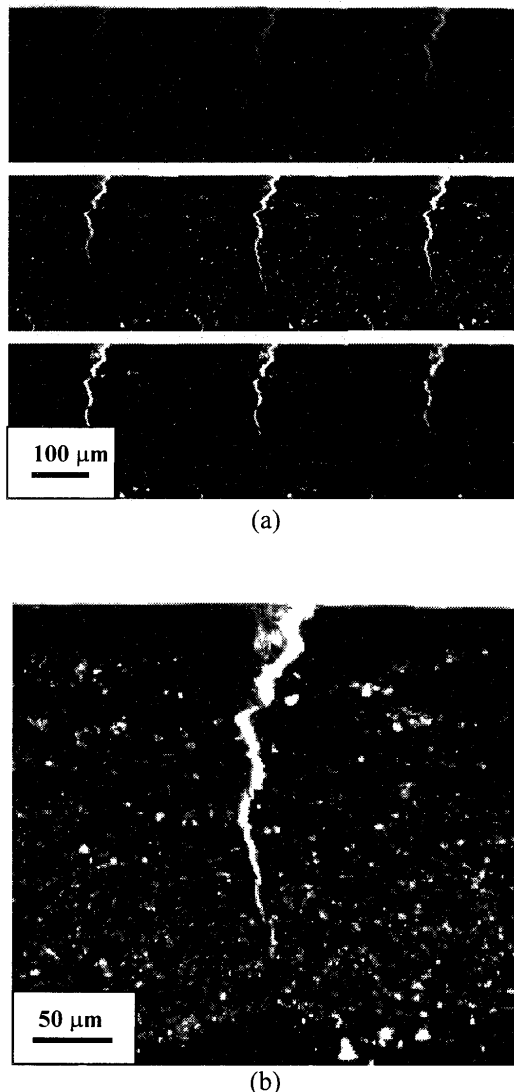

(a)

(a)

(b)

Fig. 6 (a) CLSM series of 9 x-y optical sections of laser-treated YPSZ coating (laser power: 2.0kW, beam size: □ 7 × 7mm²); (b)three-dimensional reconstruction of Fig. 6(a) corresponding to a volume of 320 by 320 by 18 μm³

(b)

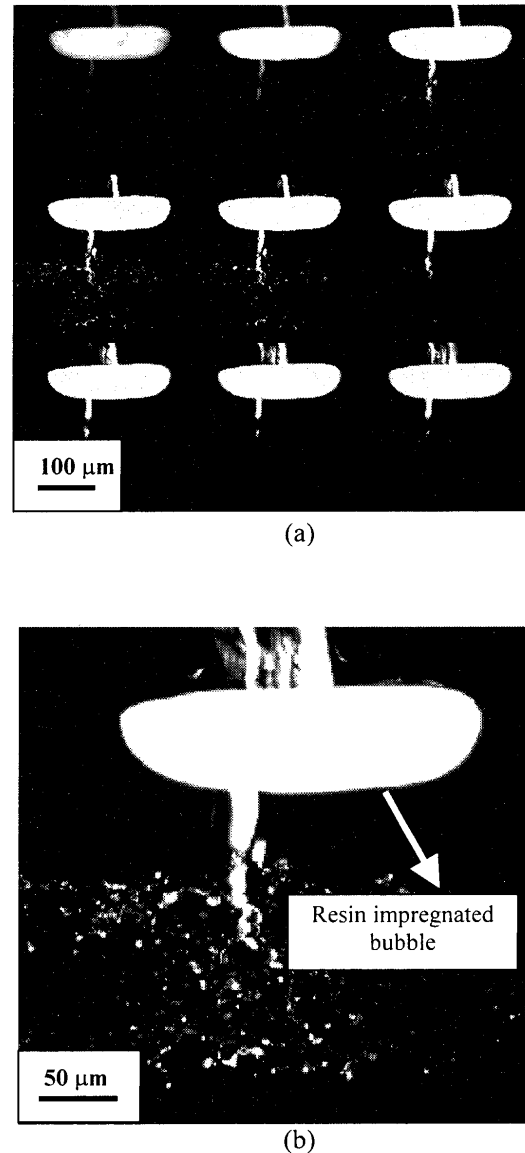**Fig. 5** (a) CLSM series of 9 x-y optical sections of laser-treated YPSZ coating (laser power: 1.5kW, beam size: □ 7 × 7mm²); (b)three-dimensional reconstruction of Fig.5(a) corresponding to a volume of 320 by 320 by 18 μm³

Microstructure observation by CLSM is very effective way of collecting three dimensional information of sprayed coatings and differentiating the original defects from ones induced by metallographical procedures. However, the resolution of CLSM is inferior to the scanning electron microscopy (SEM), so the observation of vacuum infiltrated specimen by SEM was also carried out. **Fig. 7** shows the one example of a scanning electron micrograph of YPSZ coating prepared by plasma laser hybrid spraying process (laser power: 2.5kW, beam size: □ 5 × 5mm²). In the case of coatings prepared by hybrid spraying processes, the feature of cracks in the coating was different from the post-treated coatings. From the post treatments of

coatings, sprayed coatings remelted and resulted in mainly vertical cracks which extended to the interface of bond-coat and top-coat.
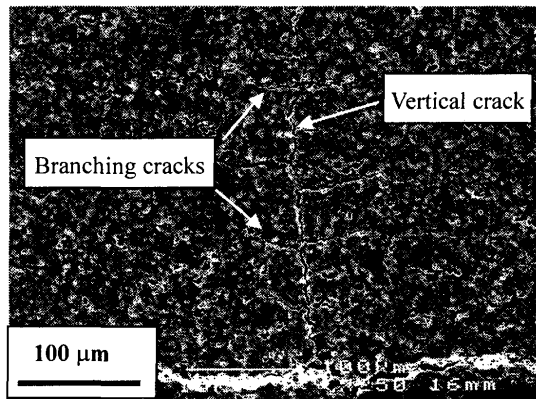

Fig. 7   Scanning electron micrograph of YPSZ coating prepared by plasma laser hybrid spraying process (laser power: 2.5kW, beam size: □5 × 5mm²)

However, the feature of cracks in the coating, prepared by hybrid spraying processes, was characterized as a feather-like structure with a significant number of branching cracks which was not observed in the post-treated coatings. During the hybrid spraying treatments, the sprayed particles were reheated by simultaneously irradiating laser and maintained at high temperature causing a gradual cooling of sprayed particles. The finely networked cracks of coatings prepared by hybrid process were considered due to the densification between sprayed splats by laser heat-treatment and retarded cooling procedure, whereas the rapid solidification of the remelted coating caused mainly vertical cracks with a broad width in post-treatment. It was also found that the branching number per vertical crack and the average length were significantly changed by the hybrid laser conditions.

Now, we are investigating the control of this segmented structure to improve the thermal shock resistance of YPSZ coating by using the plasma laser hybrid spraying process.

3.2 Thermal shock resistance of coatings prepared by post-laser treatment and plasma-laser hybrid process

Fig. 8 shows the experimental results obtained from cyclic thermal test of YPSZ coatings treated at different laser powers. As-sprayed coating failed after just three thermal cycle tests. On the other hand, the laser treated coating at 1.5kW (power density, 31W/mm²) showed a five times of improvement of thermal shock resistance compared with the as-sprayed coating. Further

increases of laser power density for laser treatment lower the lifetime in cyclic thermal shock tests. From the observation of cracks as shown in **Fig. 5** and **Fig. 6**, the depth and width of cracks and spacing between cracks appear to be a crucial parameters that influence the thermal shock resistance. When the excessively penetrated cracks exist, the thermal shock resistance of coatings suddenly drops.
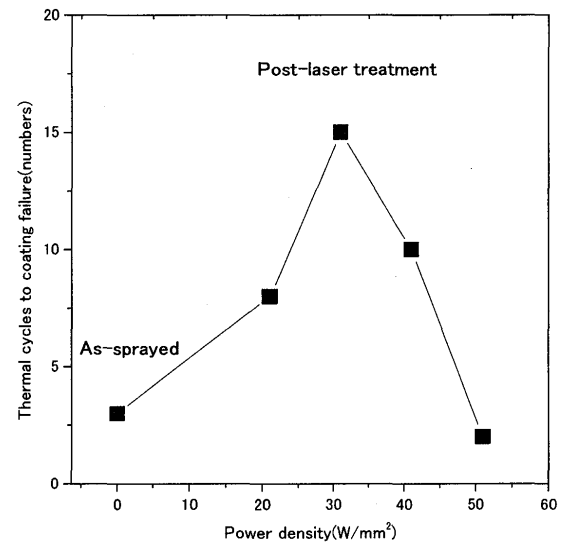

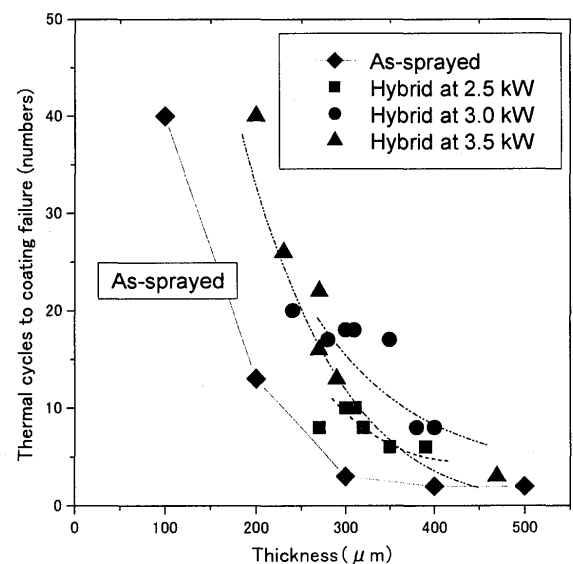Fig. 8   Cyclic thermal test results of YPSZ coatings treated at different laser powers (beam size, □7×7 mm²).

Fig. 9   Cyclic thermal test results of YPSZ coatings prepared by hybrid spraying processes (beam size, □ 5×5 mm²).

Fig. 9 shows cyclic thermal test results of YPSZ coatings prepared by hybrid spraying processes. The thermal shock resistance is a function of coating thickness, i.e., thinner coatings have a higher thermal shock resistance. When compared at the same thickness of post-treated coating of 300μm, the hybrid sprayed coatings show more improved thermal shock resistance (hybrid at 3.0kW) than post-treated coatings and a sudden drop of a thermal shock resistance was not observed, even at higher laser power (hybrid at 3.0kW). This improved thermal shock resistance is considered due to the microstructure of hybrid sprayed coatings which have a fiinely networked feather-like cracks

4. Conclusions

It was found that a technique using a low-viscosity resin with a fluorescent dye under a high vacuum was very effective for the accurate observation of the microstructure of TBC coating prepared by post laser treatments and laser hybrid spraying processes. From the observation of microstructure by CLSM, three dimensional information of coatings, treated at various conditions, was obtained.

As-sprayed coating failed after just three thermal cycle tests. On the other hand, the laser treated coating at 1.5kW (power density, $31W/mm^2$) showed five times of improved thermal shock resistance compared with as-sprayed coatings. Further increases of laser power density for laser treatment lower the lifetime in cyclic thermal shock tests. The plasma laser hybrid sprayed coatings show improved thermal shock resistance (hybrid at 3.0kW) compared with post-treated coatings and a sudden drop of a thermal shock resistance was not observed, even at higher laser power (hybrid at 3.0kW).

Now, we are investigating the control of this finely segmented structure to improve the thermal shock resistance of YPSZ coating by using the plasma laser hybrid spraying process

References

1) D. M. NISSLEY: Thermal Barrier Coating Life Modeling in Aircraft Gas Turbine Engines, Journal of Thermal Spray Technology, Vol. 6(1997), No.1, pp. 91-98.
2) J. A. HYANES, M. K. FERBER, and W. D. PORTER: Thermal Cycling Behavior of Plasma-Sprayed Thermal Barrier Coatings with Various MCrAlX Bond Coats, Journal of Thermal Spray Technology, Vol. 9(2000), No.1, pp. 38-48
3) S. STECURA: Effects of Yttrium and Chromium Concentrations in Bond Coatings on the Performance of Zirconia-Yttria Thermal Barriers, Thin Solid Films, Vol. 95(1980), pp. 481-489
4) H. L. TSAI and P. C. TSAI: Performance of Laser-glazed Plasma-Sprayed(ZrO_2-12wt.%Y_2O_3)/(Ni-22wt.%Cr-10wt. %Al-1wt.%Y)Thermal Barrier Coatings in Cyclic Oxidation Tests, Surface and Coatings Technology, Vol. 71(1995), pp. 53-59.
5) I. ZAPLATYNSKY: Performance of Laser-glazed Zirconia Thermal Barrier Coatings in Cyclic Oxidation and Corrosion Burner Rig Tests, Thin Solid Films, Vol. 95 (1982), pp. 275-284.
6) D. L. RUCKLE: Plasma-Sprayed Ceramic Thermal Barrier Coatings for Turbine Vane Platforms, Thin Solid Films, Vol. 73(1980), pp. 455-461.
7) Thermal Spray 2001: New Surface for a New Millennium, C. C. Berndt, K. A. KHOR, and E. F. LUGSCHEIDER, ed., ASM international, Materials Park, OH, USA, 2001, pp. 575-582.
8) J. KARTHIKEYAN, A. K. SINHA, and A. R. BISWAS: Impregnation of Thermally Sprayed Coatings for Microstructural Studies, Journal of Thermal Spray Technology, Vol. 5(1996), No.1, pp. 74-78.
9) A. OHMORI, Z. ZHOU, and N. EGUCHI: Hybrid Spraying of Zirconia Thermal Barrier Coating with YAG Laser Combined Plasma Beam, Trans. of Welding Research Institute of Osaka University (JWRI), Vol. 26 (1997), No.1, pp.99-107
10) N. LLORCA-LSERN, M. PUIG, and M. ESPANOL: Improving the Methodology for Coating Defects Detection, Journal of Thermal Spray Technology, Vol. 8(1999), No.1, pp. 73-78.
11) Y. FU, A. W. BATCHELOR, H. XING, and Y. GU: Wear Behavior of Laser-treated Plasma-Sprayed ZrO2 Coatings, Wear, Vol. 210(1997), pp. 157-164.